SYNTHESIS OF Al-Si-Ni NANOSTRUSTURED MATERIALS BY MECHANICAL ALLOYING

SUBMITTED BY

HEMANT KUMAR GUSAIWAL

ROLL NO. :-10504013

SRIKANTA PATTNAIK

ROLL NO. :-10504033

UNDER THE GUIDANCE OF

Dr. S. MULA

DEPARTMENT OF METALLURGICAL & MATERIALS ENGINEERING

NATIONAL INSTITUTE OF TECHNOLOGY ROURKELA

National Institute of Technology
Rourkela

CERTIFICATE

This is to certify that the thesis entitled, "**Synthesis of Al-Si-Ni nanostructured materials by Mechanical alloying**" being submitted by **Hemant Kumar Gusaiwal and Srikanta Pattanaik** to the **Metallurgical and Materials Engineering Department** at the **National Institute of Technology, Rourkela**, for the degree of **Bachelor of Technology,** is a record of bonafide research work carried out under my supervision and guidance. The result presented in this thesis has not been submitted elsewhere for the award of any Degree or Diploma.

This work, in my opinion, has reached the standard of fulfilling the requirements for the award of the degree of **Bachelor of Technology** in accordance with the regulation of the institute

Date :

(Dr. Suhrit Mula)

Dept. of Met. & Mat. Eng.
National Institute of Technology
Rourkela-769008

ACKNOWLEDGEMENT

I want to take the opportunity to extend my hearty indebtedness to my guide **S. Mula** for his invaluable guidance, patience, regular monitoring and meticulous attention at all stages during my course of work for which this work has come to fruition.

.

I express my grateful thanks to **Prof. B. B. Verma**, **Head of the Department** for providing me the necessary facilities in the Department. I am also grateful to **Prof. A. K. Panda** for their constant concern and encouragement for execution of this work.

I also express my sincere special gratitude to **Prof. S Bhattacharya**, **Head, Dept. of Ceramic Engineering** for his timely help during the characterization of some work.

I am thankful to **Sri Udayanath Sahu, Sri Rajesh Pattnaik,** Metallurgical & Materials Engineering, Technical assistants, for their co-operation in experimental work. Special thanks to **all my family members and friends** for being so supportive and helpful in every possible way.

HEMANT KUMAR GUSAIWAL

ABSTRACT

An effort has been made to synthesize Al-based nanostructure by mechanical alloying (MA). Elemental powder of Al, Si and Ni were blended to obtain nominal composition of $Al_{75}Si_{15}Ni_{10}$. Alloying was carried out in a high energy planetary ball mill using stainless steel grinding media at 300 r.p.m. up to 50 h. Toluene was used as the process control agent (PCA). The ball to powder weight ratio was maintained at 10:1. The phase evolution of the milled samples was studied by X-ray diffraction (XRD) analysis. The microstructural characterization of the milled powder was followed by scanning electron microscopy (SEM) and XRD. Dissolution of Si and Ni in Al was found to be 15% and 10% respectively along with the formation of some intermetallic phases.

SEM micrographs showed that the powder morphology was changed from coarse layered structures obtained by very short period of milling to finer as the milling time increased. XRD and energy dispersive X-ray analysis (EDX) showed the formation of a homogeneous solid solution of the above said blends after milling for 50 h. The crystallite size, lattice strain (%) and lattice parameter were calculated from major XRD peaks. It shows that the crystal size decreased very rapidly up to 25 h of milling and then slowly became almost constant with further milling, whereas, lattice strain (%) increased gradually up to 25 h very rapidly and then very slowly became nearly constant with progress of milling. This suggests that major structural changes and dissolution of the alloying elements almost completed by 25 h, and further milling refined the product by MA. The lattice microstrain of the material increases exponentially. It increases rapidly up to 25 h and then increased slowly as the milling progresses further. The change of lattice parameter of Al-rich solid solution showed a rapid decrease throughout the process of MA. This is because of the entrance of Si and Ni atoms into the lattice of the Al which causes distortion in it. The change in the above mentioned parameters were determined up to 30 h of milling as on further milling Al peaks vanishes because of formation of partially amorphous structure along with some intermetallic phases.

CONTENTS:-

CERTIFICATE 2

ACKNOWLEDGEMENT 3

ABSTRACT 4

1.0 INTRODUCTION 8

2.0 LITERATURE REVIEW 9

2.1 NANO MATERIAL 9

2.2 NANO MATERIALS VS CONVENTIONAL MATERIALS 9

2.2.1 YIELD STRENGTH 9

2.2.2 DUCTILITY 10

2.2.3 STRAIN HARDENING 11

2.2.4 STRAIN RATE SENSITIVITY 11

2.2.5 CREEP OF NANO STRUCTURE MATERIALS 12

2.2.6 FATIGUE IN NANO CRYSTALLINE MATERIALS 12

2.3 PREPARATION METHOD 13

2.3.1 INERT GAS CONDENSATION 13

2.3.2 ELECTRODEPOSITION 14

2.3.3 CRYSTALLIZATION FROM AMORPHOUS SOLIDS 14

2.3.4 SEVERE PLASTIC DEFORMATION 15

2.3.5 SOL GEL SYNTHESIS 15

2.3.6 MECHANICAL ALLOYING 16

2.3.6.1 RAW MATERIALS 17

2.3.6.2 TYPES OF MILLS 18

(a) SPEX SHAKER MILLS 18

(b) PLANETARY BALL MILLS 19

(c) ATTRITOR MILLS 20

(d) COMMERCIAL MILLS 21

2.3.6.3 PROCESS VARIABLES 22

(a) TYPES OF MILLS 22

(b) MILLING CONTAINER 23

(c) MILLING SPEED 23

(d) MILLING TIME 24

(e) GRINDING MEDIUM 24

(f) BALL TO POWDER RATIO 25

(g) EXTENT OF FILLING THE VIAL 26

(h) MILLING ATMOSPHERE 26

(i) PROCESS CONTROL AGENTS 26

(j) TEMPERATURE OF MILLING 27

2.3.6.4 MECHANISM OF ALLOYING 28

3. EXPERIMENTAL 29

3.1 SAMPLE PREPARATION 29

3.2 X-RAY DIFFRACTION (XRD) 29

3.3 SCANNING ELECTRON MICROSCOPE (SEM) 31

3.4 ENERGY DESPERSIVE X-RAYANALYSIS (EDX) 33

4. RESULT AND DISSCUSSION 34

4.1 STRUCTURAL CHARACTERISATION OF MECHANICAL ALLOYED POWDERS BY XRD ANALYSIS 34

4.2 MORPHOLOGY OF POWDERED USING SEM 38

4.3 EDX ANALYSIS 40

5. CONCLUSION 41

5.1 SCOPE OF FUTURE WORK 41

REFRENCES 42

1: **INTRODUCTION :**

Nanomaterials have been the subject of widespread research over the past couple of decades with significant advancement in their understanding especially in last few years [1]. As the name suggests they are single or multiphased polycrystals with size range of order <100 nm. Nanomaterials are characterised by some excellent mechanical properties than conventional coarse grain materials.

Generally nanomaterials exhibit high strength properties. As the grain size decreased, an increasing fraction of atoms can be ascribed to the grain boundaries. As the grain boundaries act as pinning points for dislocation movement, its increase in density helps in strengthening the structure hence increases the yield strength of the material [2]. Nanomaterials exhibit improved toughness, enhanced diffusivity, higher specific heat, enhanced thermal coefficient, superior magnetic properties.

The starting point for the development of new high strength Al-alloys was the discovery of high tensile strength exceeding 1200 MPa for melt-spun Al-ETM-LTM amorphous ribbons [3]. Such strength levels are twice as high as for conventional crystalline alloys. Generally Al-alloys are preferred because of its combination of light weight with excellent yield strength [4]. It has corrosion resistance properties because of formation of aluminium oxide on the surface [4]. Another interesting materials, consisting of a nanoscale phase mixture of quasicrystalline particles, coexisting with a ductile FCC Al-phase, has been produced in various melt-spun Al-based ribbons [5]. This type of mixed structures exhibit good ductility and high temperature tensile strength about 100-1340MPa [5]. The quasicrystals act as strength bearing component, while Al-matrix supplies ductility.

During past decades great efforts have been devoted to the research of rapidly solidified (RS) aluminium alloys [6].Particularly, RS multicomponent Al-TM(TM-Transition metals) alloys have been studied extensively. Some Al-Si alloys show moderate strength levels (300MPa) and a low thermal stability. Al alloys containing Silicon, a rare earth material, and Nickel, a late transition metal, combine high tensile strength and good wear resistance [7]. Some researches have already been performed by Jerzy Latuch, Grzegorz Cieslak, Tadeusz Kulik (Warsaw university of Technology) on fabrication of bulk nanocrystalline Al-Si-Ni alloys produced by ball milling of rapidly solidifies ribbons followed by hot isostatic pressing [8] for high strength applications [9].

The aim of the present work is to synthesize Al-Si-Ni nanostructured material by mechanical alloying and characterisation of the product.

Objectives and Scope of Present Study:

- Synthesize Al based alloy having compositions Al75Si15Ni10 by MA.
- Characterization of the powder products by XRD analysis.
- Characterization of the powder products by SEM and EDX analysis.
- Finally, correlate the structures and properties.

2: LITERATURE REVIEW:-

2.1 *Nano material:*

Nanomaterials are defined as the materials having size order in a range of 1-200nm.They are applications with morphological features smaller than a one tenth of a micrometer in at least one dimension [10]. A logical definition would situate the nanoscale between micro scale (0.1µm) and molecular/atomic scale (0.2µm). Nanomaterials are widely accepted as it miniaturizes the structure providing some excellent properties compared to conventional coarser materials.

Nanomaterials have been classified on different basis e.g. Siegel classified nanostructured materials into four categories according to dimensionality i.e. 0D-nanoclusters; 1D-multilayers; 2D-nanogra-ned layers; 3D-equiaxed bulk solids. Classification is also based on the grain size. Gieter classified according to morphology and distribuition of nanocrystalline component. According to shape of the crystallities, crys-three categories of nanomaterials may be distinguished; layer shaped tallities, rod shaped crystallities and nanostructures composed of equiaxed nanometer sized crystallites.

2.2 Nanomaterials Vs Conventional materials:

Nanomaterials are dominating the conventional coarser materials because its wide range of advantages as they exhibit some excellent mechanical properties along with miniaturizing the structure. Mechanical properties i.e. yield stress, ductility, strain hardening, strain sensitivity, dynamic response, creep, fatigue, temperature stability etc.

2.2.1 Yield strength: Grain size is known to have significant effect on the mechanical properties, in particular, the yield stress. The dependence of yield stress in the

conventional polycrystalline range. Yield stress, σ_y, for materials with grain size d, is found to follow the Hall-Patch relation.

$$\sigma_y = \sigma_o + K/\sqrt{d}$$

Where, σ_o is the friction stress and K is a material constant called strengthening co-efficient. This is indeed an approximation to keep the power in a range of 0.3-0.7.The smaller is the grain size, more will be the number of grains, hence the strength of material increases as grain boundaries act as pinning points for dislocations. Since the lattice structure of adjacent grains differs in orientation, it requires more energy for a dislocation from moving in a continuous slip plane. Impeding this dislocation movement will hinder the onset of plasticity and hence increase the yield strength [10]. The grain boundary is also much more disorder than inside the grain which also prevents the dislocation from moving in a continuous slip plane. The mechanical properties of FCC metals with nano-range grain sizes have been estimated from uniaxial tension/compression test and nano-indentation. Often micro size tensile specimens are used to a- void the influence of imperfections [11] e.g. voids that might adversely influence the mechanical response of the material.

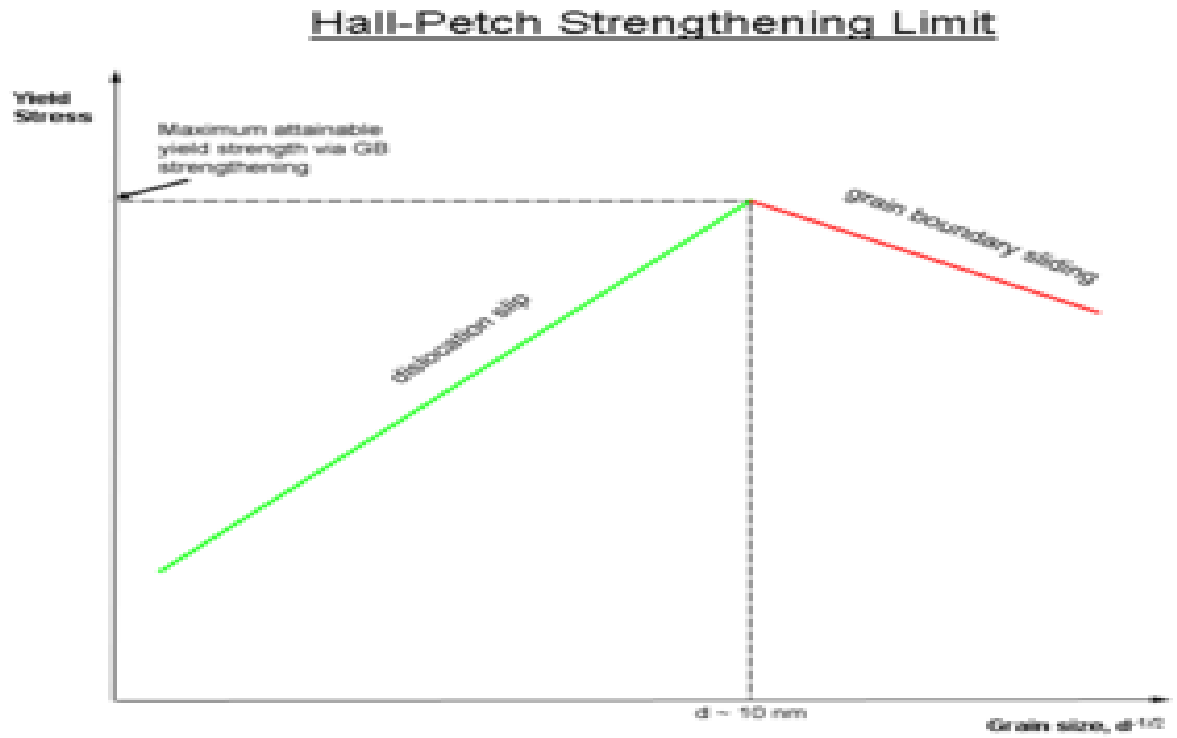

Fig 1: Hall-Petch strengthening limit by size of dislocations.

2.2.2 Ductility: In the conventional grain size regime, usually a reduction in grain size leads to an increase in ductility. Thus one should expect a ductility increase as the grain size is reduced to nanoscale. However, the ductility is small for the most grain sizes <25mm for metals that in the conventional grain size have tensile ductilities of 40-60% elongation. Koch identified three major sources of limited ductility in nano-crystalline materials, namely; (i)articrafts from processing; (ii)tensile instability; (iii)crack nucleation or shear instability. It is difficult to process nanostructured materials free from the articrafts that mask the inherent mechanical properties. As a result, molecular dynamics simulation has been considered to be a valuable tool in aiding our understanding of their deformation mechanism [12].The result of atomic simulations have allowed several investigators to suggest different plastic deformation mechanisms as a function of grain size [13].There seems to be a agreement in this existence of three regimes: (a) grain size d<1µm regime in which unit dislocations and work hardening control plasticity; (b)smallest grain size d<10nm regime, where limited intragranular dislocation activity occurs and grain boundary shear is believed to be the mechanism of deformation. The intermediate grain size regime i.e. 10nm-1µm is less well understood. These mechanisms are thought to be affecting ductility significantly.

2.2.3 Strain Hardening: Nanocrysalline and ultrafine grained materials cannot generally sustain uniform tensile elongation. Several reports virtually no strain hardening after an initial stage of rapid strain hardening over a small plastic strain regime (1-3%) which is different from the response of coarse grained polycrystalline metals [12].

The density of dislocations in a nanocrystalline sample saturates due to dynamic recovery or due to the annihilation of dislocations into the grain boundaries. It is only during large additional strain that work hardening is observed. Dynamic recovery is known to occur during severe plastic deformation [14]. Due to the rise in the temperature, recovery converts the deformed microstructure into ultra.ne grains having both low-angle and high-angle grain boundaries. Low strain hardening behavior has been observed for samples processed by both equal angular channel pressing and powder consolidation [14].

The stress–strain response of a nanocrystalline metal, e.g. copper under tension shows a rapid peak and subsequent softening due largely to necking. The absence of strain hardening (dr/de = 0) causes localized deformation leading to low ductility. Flat compression curves have also been observed for other nanocrystalline metals including Fe (BCC) and Ti (HCP) [14]. Necking is observed in most cases with the severe case of instability, and shear bands form in the consolidated Fe [15].

2.2.4 Strain Rate Sensitivity: There have been reports of both increased and decreased strain rate sensitivity with decreasing grain size in metals. Iron, which is normally rate sensitive, with a strain rate exponent '*m'*. Hardening exponent on the order of 0.04, goes

down in the value to 0.004 when the grain size is 80 nm. Malow et al. prepared nanocrystalline Fe using ball milling and consolidation, and found a low m 0.006 at d 20 nm. An opposite e.ect was found by Gray et al. on ultrafine grained FCC metals produced by ECAP: Cu, Ni and Al–4Cu 0.5Zr. Their mechanical response was found to depend on the applied strain rate, which ranged from 0.001 to 4000 s 1.The strain rate sensitivity, m, based on the above strain rate range, was measured to be 0.015 for Cu, 0.006 for Ni and 0.005 for Al–4Cu–0.5 Zr. Gray et al. Stress–strain response of ultra.ne grained: (a) Cu, (b) Ni. Relatively high rate sensitivity, coupled with the nearly zero post-yield work hardening rates in the ultra fine grained Cu and Ni, to a high pre-existing dislocation density.

2.2.5Creep of Nanocrystalline Materials: Creep in coarse grained materials has been widely studied for approximately one century and accurate models exist that capture deformation features and explain mechanisms involved therein. Creep in nanocrystalline materials has been studied only in recent years owing to several complications involved. First of all is the limitation of synthesizing bulk nanomaterial free of defects (porosity and impurities) with uniform grain size distribution that could provide reliable data to explain the deformation process. Second is the significant increase in the volume fraction of grain boundaries and intercrystalline defects such as triple lines and quadruple junctions that renders the creep mechanism complicated and leads to associated challenges in developing a model that could explain the deformation process. Third, grain growth occurs at much lower temperature as compared to coarse grained materials limiting the testing temperatures to a low fraction of the melting point. Since the volume fraction of grain boundaries is high, diffusion creep is considered to be significant. The high temperature deformation of crystalline materials is given by the following (Bird–Dorn–Mukherjee) equation:

$$Є=ADGb/kT\ (b/d)^{p}\ (\partial/G)^{n}$$

Where, ϵ is the strain rate, A is a dimensionless constant, G is the shear modulus, b is the magnitude of the Burgers vector, k is Boltzmann's constant, T is the absolute temperature, p is the inverse grain size exponent, and n is the stress exponent. Among the established diffusional creep mechanisms in coarse grained materials are the Nabarro–Herring creep that involves vacancy flow through the lattice and Coble creep that involves vacancy flow along the grain boundaries.

2.2.6 Fatigue in Nanocrystalline materials: There have not been many reports on the fatigue properties of nanocrystalline materials. Among the earliest study is Whitney et al. [16] on tension–tension cycling of nanocrystalline copper prepared by inert gas condensation, with a maximum stress that ranged from 50% to 80% of the yield stress. The

minimum stress was 10MPa. After several hundred thousand cycles, a moderate increase in grain size was observed (approximately 30%). The samples were shown to elongate slightly in the course of a prolonged fatigue test. The amount of strain is similar to the room temperature creep strain observed previously in nanocrystalline copper under a constant stress comparable to the maximum cyclic stress. The cyclic deformation appeared to be elastic. However, an elastic modulus was measured that is a factor of 2 smaller than the modulus for ordinary copper.

2.3 PREPARATION METHODS :

2.3.1 Inert Gas Condensation : The inert gas condensation technique, conceived by Gleiter [17], consists of evaporating a metal (by resistive heating, radio-frequency, heating, sputtering, electron beam heating, laser/plasma heating, or ion sputtering) inside a chamber that is evacuated to a very high vacuum of about 10_7 Torr and then backfilled with a low-pressure inert gas like helium. The evaporated atoms collide with the gas atoms inside the chamber, lose their kinetic energy, and condense in the form of small particles. Convection currents, generated by the heating of the inert gas by the evaporation source and by the cooling of the liquid nitrogen-filled collection device (cold finger) carry the condensed fine powders to the collector device. The deposit is scraped off into a compaction device. Compaction is carried out in two stages: (a) low pressure compacted pellet; (b) high pressure vacuum compaction. The scraping and compaction processes are carried out under ultrahigh vacuum conditions to maintain the cleanliness of the particle surfaces and to minimize the amount of trapped gases. The inert gas condensation method produces equiaxed (3D) crystallites. The crystal size of the powder is typically a few nanometers and the size distribution is narrow. The crystal size is dependent upon the inert gas pressure, the evaporation rate, and the gas composition. Extremely .ne particles can be produced by decreasing either the gas pressure in the chamber or the evaporation rate and by using light rather than heavy inert gases (such as Xe). A great deal of the early work on mechanical properties of nanocrystalline materials used the inert gas condensation technique. One shortcoming is the possibility of contamination of powders and porosity due to insufficient consolidation. There is also the possibility of imperfect bonding between particles, since most of the early work used cold consolidation. Nevertheless, the results obtained using specimens prepared by this method led the foundation of our understanding. The important contributions of Weertman, Siegel, and coworkers [18] have used materials produced by this method. They were the first systematic studies on the mechanical properties of nanocrystalline

metals (Cu and Pd) and were initiated in 1989. Nanocrystalline alloys can also be synthesized by evaporating the different metals from more than one evaporation source. Rotation of the cold finger helps in achieving a better mixing of the vapor. Oxides, nitrides, carbides, etc. of the metals can be synthesized by filling the chamber with oxygen or nitrogen gases or by maintaining a carbonaceous atmosphere. Additionally, at small enough particle sizes, metastable phases are also produced.

Thus, this method allows the synthesis of a variety of nanocrystalline materials. The peak densities of the as-compacted metal samples have been measured with values of about 98.5% of bulk density. However, it has been established that porosity has a profound effect on the mechanical strength, especially in tension.

2.3.2 Electrodeposition: The electrodeposition technique has significant advantages over other methods for synthesizing nanocrystalline materials: (1) potential of synthesizing large variety of nanograin. Materials—pure metals, alloys and composite systems with grain sizes as small as 20 nm,(2) low investment, (3) high production rates, (4) few size and shape limitations, and (5)high probability of transferring this technology to existing electroplating and electroforming industries.

Over the past few years, Erbetal [19] have studied the synthesis, structure and properties of nanocrystalline nickel synthesized by pulse electrodeposition. They demonstrated that grain refinement of electroplated nickel into the nanometer range results in unique and, in many cases, improved properties as compared to conventional polycrystalline nickel. Electrodeposition of multilayered (1D) metals can be achieved using either two separate electrolytes or much more conveniently using one electrolyte by appropriate control of agitation and the electrical conditions. Also, 3D nanostructure crystallites can be prepared using this method by utilizing the interface of one ion with the deposition of the other. It has been shown that electrodeposition yields grain sizes in the nanometer range when the electrodeposition variables are chosen such that nucleation of new grains is favored rather than growth of existing grains. This was achieved by using high deposition rates, formation of appropriate complexes in bath, addition of suitable surface-active elements to reduce surface diffusion of ad-atoms, etc. This technique can yield porosity-free finished products that do not require subsequent consolidation processing. Furthermore, this process requires low capital investment and provides high production rates with few shape and size limitations. This high annealing twin density is responsible for the enhancement of ductility which will be discussed later.

2.3.3 Crystallization from amorphous solids: The basic principle for the crystallization method from the amorphous state [20] is to control the crystallization kinetics by optimizing the heat treatment conditions so that the amorphous phase crystallizes completely into a polycrystalline material with ultrafine crystallites. The metallic glasses can be prepared by means of the existing routes, such as melt-spinning, splat-quenching, mechanical alloying, vapor

deposition, or electrodeposition. Crystallization of amorphous solids has been successfully applied in producing nanometer-sized polycrystalline materials in various alloy systems, e.g., in Fe-, Ni-, and Co-based alloys, as well as some elements. The complete crystallization of amorphous solids is a promising method for the synthesis of nanocrystalline materials because it possesses some unique advantages, the most important being porosity-free product and the ease of synthesizing nanocrystalline, intermetallics, supersaturated metallic solid solutions, and composites. The amorphous solids are in thermodynamic metastable states and they transfer into more stable states under appropriate circumstances. The driving force for the crystallization is the difference in the Gibbs free energy between the amorphous and crystalline states. Usually, amorphous solids may crystallize into polycrystalline phases when they are subjected to heat treatment, irradiation, or even mechanical attrition. Of these techniques, conventional thermal annealing is most commonly utilized in investigations of amorphous solids.

2.3.4 Severe Plastic deformation: Severe plastic deformation breaks down the microstructure into finer and finer grains. As early as 1960, Langford and Cohen and Rack and Cohen [21] demonstrated that the microstructure in Fe–0.003%C subjected to high strains by wire drawing exhibited sub grain sizes in the 200–500 nm range. The use of severe plastic deformation (SPD) for the processing of bulk ultra.ne-grained materials is now widespread [22]. Again, this is not a new technology, since piano wire, known for over a century, owes its strength to an ultrafine grain size. Although any means of introducing large plastic strains in metals may lead to the reduction of the grain size, two principal methods for subjecting a material to severe plastic deformation have gained acceptance: these are known as equal-channel angular pressing (ECAP) and high-pressure torsion (HPT).

2.3.5 Sol gel Synthesis: The sol-gel process is a wet-chemical technique (chemical solution deposition) widely used recently in the fields of materials science and ceramic engineering. Such methods are used primarily for the fabrication of materials (typically a metal oxide) starting from a chemical solution which acts as the precursor for an integrated network (or gel) of either discrete particles or network polymers. Typical precursors are metal alkoxides and metal chlorides, which undergo various forms of hydrolysis and polycondensation reactions. The formation of a metal oxide involves connecting the metal centers with oxo (M-O-M) or hydroxo (M-OH-M) bridges, therefore generating metal-oxo or metal-hydroxo polymers in solution. Thus, the sol evolves towards the formation of a gel-like diphasic system containing both a liquid phase and solid phase whose morphologies range from discrete particles to continuous polymer networks.

In the case of the colloid, the volume fraction of particles (or particle density) may be so low that a significant amount of fluid may need to be removed initially for the gel-like properties to be recognized. This can be accomplished in any number of ways. The simplest

method is to allow time for sedimentation to occur, and then pour off the remaining liquid. Centrifugation can also be used to accelerate the process of phase separation.

Removal of the remaining liquid (solvent) phase requires a drying process, which is typically accompanied by a significant amount of shrinkage and densification. The rate at which the solvent can be removed is ultimately determined by the distribution of porosity in the gel. The ultimate microstructure of the final component will clearly be strongly influenced by changes imposed upon the structural template during this phase of processing. Afterwards, a thermal treatment, or firing process, is often necessary in order to favor further polycondensation and enhance mechanical properties and structural stability via final sintering, densification and grain growth. One of the distinct advantages of using this methodology as opposed to the more traditional processing techniques is that densification is often achieved at a much lower temperature.

The precursor sol can be either deposited on a substrate to form a film (e.g., by dip coating or spin coating), cast into a suitable container with the desired shape (e.g., to obtain monolithic ceramics, glasses, fibers, membranes, aerogels), or used to synthesize powders (e.g., microspheres, nanospheres). The sol gel approach is a cheap and low-temperature technique that allows for the fine control of the product's chemical composition. Even small quantities of dopants, such as organic dyes and rare earth elements, can be introduced in the sol and end up in uniformly dispersed in the final product. It can be used in ceramics processing and manufacturing as an investment casting material, or as a means of producing very thin films of metal oxides for various purposes. Sol-gel derived materials have diverse applications in optics, electronics, energy, space, (bio)sensors, medicine (e.g., controlled drug release), reactive material and separation (e.g., chromatography) technology.

The interest in sol-gel processing can be traced back in the mid-1880s with the observation that the hydrolysis of tetraethyl orthosilicate (TEOS) under acidic conditions led to the formation of SiO_2 in the form of fibers and monoliths.

2.3.6 Mechanical alloying:

Scientific investigations by materials scientists have been continuously directed towards improving the properties and performance of materials. Significant improvements in mechanical, chemical, and physical properties have been achieved through chemistry modifications and conventional thermal, mechanical, and thermo mechanical processing methods. However, the ever-increasing demands for ``hotter, stronger, stiffer, and lighter" than traditional materials have led to the design and development of advanced materials. The high-technology industries have given an added stimulus to these efforts. Advanced materials may be defined as those where first consideration is given to the systematic synthesis and control of the structure of the materials in order to provide a precisely tailored set of properties for demanding applications [23]. It is now well recognized that the structure and

constitution of advanced materials can be better controlled by processing them under non-equilibrium (or far-from-equilibrium) conditions. Amongst many such processes, which are in commercial use, rapid solidification from the liquid state, mechanical alloying, plasma processing, and vapor deposition have been receiving serious attention from researchers. The central underlying theme in all these techniques is to synthesize materials in a non-equilibrium state by ``energizing and quenching". The energization involves bringing the material into a highly non-equilibrium (metastable) state by some external dynamical forcing, e.g., through melting, evaporation, irradiation, application of pressure, or storing of mechanical energy by plastic deformation. Such materials are referred to as ``driven materials" by Martin and Bellon [24]. The energization may also usually involve a possible change of state from the solid to liquid or gas. The material is then quenched into a configurationally frozen state, which can then be used as a precursor to obtain the desired chemical constitution and/or microstructure by subsequent heat treatment/processing. It has been shown that materials processed this way possess improved physical and mechanical characteristics in comparison with conventional ingot (solidification) processed materials.

Process of mechanical alloying: The actual process of MA starts with mixing of the powders in the right proportion & loading the powder mix into the mill along with the grinding medium (generally steel balls). This mix is then milled for the desired length of time until a steady state is reached when the composition of every powder particle is the same as the proportion of the elements in the starting powder mix. The milled powder is then consolidated into a bulk shape and heat treated to obtain the desired microstructure and properties. Thus the important components of the MA process are the raw materials, the mill, and the process variables. We will now discuss the different parameters involved in the selection of raw materials, types of mills, and process variables.

2.3.6.1. Raw Materials: The raw materials used for MA are widely available commercially pure powders that have particle sizes in the range of 1±200 mm. But, the powder particle size is not very critical, except that it should be smaller than the grinding ball size. This is because the powder particle size decreases exponentially with time and reaches a small value of a few microns only after a few minutes of milling. The raw powders fall into the broad categories of pure metals, master alloys, prealloyed powders, and refractory compounds. Dispersion strengthened materials usually contain additions of carbides, nitrides, and oxides. Oxides are the most common and these alloys are known as oxide-dispersion strengthened (ODS) materials. In the early days of MA, the powder charge consisted of at least 15 vol% of a ductile compressibly deformable metal powder to act as a host or a binder. However, in recent years, mixtures of fully brittle materials have been milled successfully resulting in alloy formation. Thus, the requirement of having a ductile metal. Powder during milling is no longer necessary. Accordingly, ductile-ductile, ductile-brittle, and brittle-brittle powder mixtures are

milled to produce novel alloys. Mixtures of solid powder particles and liquids have also been milled in recent times [25]. Occasionally, metal powders are milled with a liquid medium and this is referred to as wet grinding; if no liquid is involved then it is referred to as dry grinding. (Cryomilling also is wet grinding if the liquid used is at cryogenic temperatures). It has been reported that wet grinding is a more suitable method than dry grinding to obtain finer-ground products because the solvent molecules are adsorbed on the newly formed surfaces of the particles and lower their surface energy. The less-agglomerated condition of the powder particles in the wet condition is also a useful factor. It has been reported that the rate of amorphization is faster during wet grinding than during dry grinding. A disadvantage of the wet grinding, however, is the increased contamination of the powder. Thus, most of the MA/MM operations have been carried out dry. Additionally, dry grinding has been found to be more efficient than wet grinding in the decomposition of Cu(OH)2 to Cu.

2.3.6.2. Types of Mills: Different types of high-energy milling equipment are used to produce mechanically alloyed powders. They differ in their capacity, efficiency of milling and additional arrangements for cooling, heating, etc.

(a)SPEX Shaker Mills: Shaker mills such as SPEX mills, which mill about 10-20 g of the powder at a time, are most commonly used for laboratory investigations and for alloy screening purposes. These mills are manufactured by SPEX CertPrep, Metuchen, NJ. The common variety of the mill has one vial, containing the sample and grinding balls, secured in the clamp and swung energetically back and forth several thousand times a minute. The back-and-forth shaking motion is combined with lateral movements of the ends of the vial, so that the vial appears to be describing in the figure or infinity sign as it moves. With each swing of the vial the balls impact against the sample and the end of the vial, both milling and mixing the sample. Because of the amplitude (about 5 cm) and speed (about 1200rpm) of the clamp motion, the ball velocities are high (on the order of 5 m/s) and consequently the force of the ball's impact is unusually great. Therefore, these mills can be considered as high-energy variety. The most recent design of the mills has provision for simultaneously milling the powder in two vials to increase the throughput. This machine incorporates forced cooling to permit extended milling times. A variety of vial materials is available for the SPEX mills and these include hardened steel, alumina, tungsten carbide, zirconia, stainless steel, silicon nitride, agate, plastic, and methacrylate.

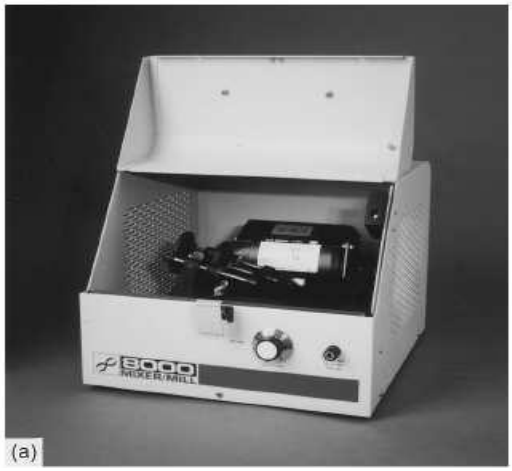

(b)Planetary ball mills: Another popular mill for conducting MA experiments is the planetary ball mill(referred to as Pulverisette) in which a few hundred grams of the powder can be milled at a time These are manufactured by Fritsch GmbH in Germany and marketed by Gilson Co., in the US and Canada. The planetary ball mill owes its name to the planet-like movement of its vials. These are arranged on a rotating support disk and a special drive mechanism causes them to rotate around their own axes. The centrifugal force produced by the vials rotating around their own axes and that produced by the rotating support disk both act on the vial contents, consisting of material to be ground and the grinding balls. Since the vials and the supporting disk rotate in opposite directions, the centrifugal forces alternately act in like and opposite directions. This causes the grinding balls to run down the inside wall of the vial-the friction effect, followed by the material being ground and grinding balls lifting off and traveling freely through the inner chamber of the vial and colliding against the opposing inside wall-the impact effect. Even though the disk and the vial rotation speeds could not be independently controlled in the earlier versions, it is possible to do so in the modern versions. In a single mill one can have either two (Pulverisette 5 or 7) or four (Pulverisette 5) milling stations. Recently, a single-station mill was also developed (Pulverisette 6).Grinding vials and balls are available in eight different materials-agate, silicon nitride, sintered corundum, zirconia, chrome steel, Cr-Ni steel, tungsten carbide and plastic polyamide. Even though the linear velocity of the balls in this type of mill is higher than that in the SPEX mills, the frequency of impacts is much more in the SPEX mills. Hence, in comparison to SPEX mills, Fritsch Pulverisette can be considered lower energy mills.

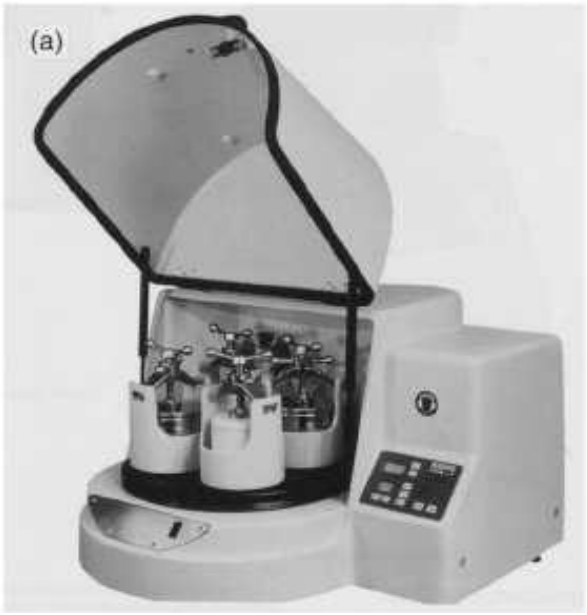

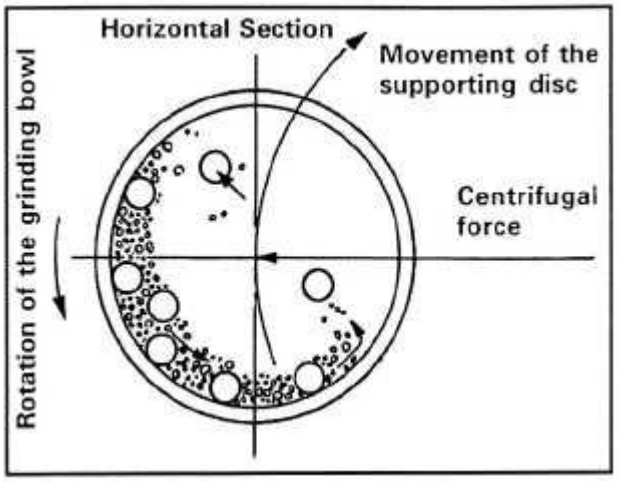

Fig:-Showing types of forces acting

(c) Attritor mills: A conventional ball mill consists of a rotating horizontal drum half-filled with small steel balls. As the drum rotates the balls drop on the metal powder that is being ground and the rate of grinding increases with the speed of rotation. At high speeds, however, the centrifugal force acting on the steel balls exceeds the force of gravity, and the balls are pinned to the wall of the drum. At this point the grinding action stops. An attritor (a ball mill capable of generating higher energies) consists of a vertical drum with a series of impellers inside it. Set progressively at right angles to each other, the impellers energize the ball charge, causing powder size reduction because of impact between balls, between balls and container

wall, and between balls, agitator shaft, and impellers. Some size reduction appears to take place by interparticle collisions and by ball sliding. A powerful motor rotates the impellers, which in turn agitate the steel balls in the drum. Attritors are the mills in which large quantities of powder (from about 0.5 to 40kg) can be milled at a time. Commercial attritors are available from Union Process, Akron, OH. The velocity of the grinding medium is much lower (about 0.5 m/s) than in Fritsch or SPEX mills and consequently the energy of the attritors is low. Attritors of different sizes and capacities are available. The grinding tanks or containers are available either in stainless steel or stainless steel coated inside with alumina, silicon carbide, silicon nitride, zirconia, rubber, and polyurethane. A variety of grinding media also is available-glass, flint stones, steatite ceramic, mullite, silicon carbide, silicon nitride, sialon, alumina, zirconium silicate, zirconia, stainless steel, carbon steel, chrome steel, and tungsten carbide. The operation of an attritor is simple. The powder to be milled is placed in a stationary tank with the grinding media. This mixture is then agitated by a shaft with arms, rotating at a high speed of about 250 rpm. This causes the media to exert both shearing and impact forces on the material. The laboratory attritor works up to 10 times faster than conventional ball mills.

(d) Commercial mills: Commercial mills for MA are much larger in size than the mills described above and can process several hundred pounds at a time. Mechanical alloying for commercial production is carried out in ball mills of up to about 3000 lb (1250kg) capacity. The milling time decreases with an increase in the energy of the mill. It has been reported that 20 min of milling in a SPEX mill is equivalent to 20h of milling in a low-energy mill of the type Invicta BX 920/2. As a rule of thumb, it can be estimated that a process that

takes only a few minutes in the SPEX mill may take hours in an attritor and a few days in a commercial mill even though the details can be different depending on the efficiency of the different mills.

2.3.6.3. Process Variables: Mechanical alloying is a complex process and hence involves optimization of a number of variables to achieve the desired product phase and/or microstructure. Some of the important parameters that have an effect on the final constitution of the powder are:

. Type of mill,
. Milling container,
. Milling speed,
. Milling time,
. Type, size, and size distribution of the grinding medium,
. Ball-to-powder weight ratio,
. Extent of filling the vial,
. Milling atmosphere,
. Process control agent, and
. Temperature of milling.

All these process variables are not completely independent. For example, the optimum milling time depends on the type of mill, size of the grinding medium, temperature of milling, ball-to-powder ratio, etc. Even then, we will discuss, in the following paragraphs, the effect of these variables (Assuming mostly that other variables have no significant effect on the specific variable being discussed) on the final product obtained after MA.

(a)Type of mill: As described above there are a number of different types of mills for conducting MA. These mills differ in their capacity, speed of operation, and their ability to control the operation by varying the temperature of milling and the extent of minimizing the contamination of the powders. Depending on the type of powder, the quantity of the powder, and the final constitution required, a suitable mill can be chosen. Most commonly, however, the SPEX shaker mills are used for alloy screening purposes. The Fritsch Pulverisette planetary ball mills or the attritors are used to produce large quantities of the milled powder. Specially designed mills are used for specific applications.

(b) Milling container: The material used for the milling container (grinding vessel, vial, jar, or bowl are some of the other terms used) is important since due to impact of the grinding medium on the inner walls of the container, some material will be dislodged and get

annealing formed either V2C or a mixture of V + VC incorporated into the powder. This can contaminate the powder or alter the chemistry of the powder. If the material of the grinding vessel is different from that of the powder, then the powder may be contaminated with the grinding vessel material. On the other hand, if the two materials are the same, then the chemistry may be altered unless proper precautions are taken to compensate for the additional amount of the element incorporated into the powder. Hardened steel, tool steel, hardened chromium steel, tempered steel, stainless steel, WC-Co, WC lined steel [26], and bearing steel are the most common types of materials used for the grinding vessels. Some specific materials are used for specialized purposes; these include copper, titanium sintered corundum, yttria-stabilized zirconia (YSZ), partially stabilized zirconia + yttria, sapphire, agate, hard porcelain, Si3N4, and Cu-Be. The shape of the container also seems to be important, especially the internal design of the container. Both flat-ended and round-ended SPEX mill containers have been used. Alloying was found to occur at significantly higher rates in the flat-ended vial than in the round-ended container. The time required to reach a constant intensity and shape of the (111) peak in the X-ray diffraction pattern of the Si-Ge mixture was 9 h for the flat-ended vial and 15 h in the round-ended vial.

(c)Milling speed: It is easy to realize that the faster the mill rotates the higher would be the energy input into the powder. But, depending on the design of the mill there are certain limitations to the maximum speed that could be employed. For example, in a conventional ball mill increasing the speed of rotation will increase the speed with which the balls move. Above a critical speed, the balls will be pinned to the inner walls of the vial and do not fall down to exert any impact force. Therefore, the maximum speed should be just below this critical value so that the balls fall down from the maximum height to produce the maximum collision energy. Another limitation to the maximum speed is that at high speeds (or intensity of milling), the temperature of the vial may reach a high value. This may be advantageous in some cases where diffusion is required to promote homogenization and/or alloying in the powders. But, in some cases, this increase in temperature may be a disadvantage because the increased temperature accelerates the transformation process and results in the decomposition of supersaturated solid solutions or other metastable phases formed during milling [27]. Additionally, the high temperatures generated may also contaminate the powders. It has been reported that during nanocrystal formation, the average crystal size increases and the internal strain decreases at higher milling intensities due to the enhanced dynamical recrystallization. The maximum temperature reached is different in different types of mills and the values vary widely. Calka et al. [28] reported that when vanadium and carbon powders were milled together at different energy levels (by adjusting the positions of the magnets in the Uni-Ball mill), the final constitution of the powder was different. For example, at very low milling energy (or speed), the powder consisted of nanometer-sized grains of vanadium and amorphous carbon, which on. At intermediate energy level, the as milled powder contained a nanostructure, which on annealing

transformed to VC. At the highest energy level, the VC formed directly on milling. Similarly, a fully amorphous phase formed in a Ni-Zr powder mixture at high energy of milling whereas a mixture of crystalline and amorphous phases formed at low and intermediate milling energies [29].

(c) Milling time: The time of milling is the most important parameter. Normally the time is so chosen as to achieve a steady state between the fracturing and cold welding of the powder particles. The times required vary depending on the type of mill used, the intensity of milling, the ball-to-powder ratio, and the temperature of milling. These times have to be decided for each combination of the above parameters and for the particular powder system. But, it should be realized that the level of contamination increases and some undesirable phases form if the powder is milled for times longer than required. Therefore, it is desirable that the powder is milled just for the required duration and not any longer.

(d)Grinding medium: Hardened steel, tool steel, hardened chromium steel, tempered steel, stainless steel, WC-Co, and bearing steel are the most common types of materials used for the grinding medium. The density of the grinding medium should be high enough so that the balls create enough impact force on the powder. However, as in the case of the grinding vessel, some special materials are used for the grinding medium and these include copper, titanium, niobium, zirconia (ZrO_2), agate, yttria stabilized zirconia (YSZ), partially stabilized zirconia + yttria, sapphire, silicon nitride (Si_3N_4), and Cu-Be. It is always desirable, whenever possible, to have the grinding vessel and the grinding medium made of the same material as the powder being milled to avoid cross contamination. The size of the grinding medium also has an influence on the milling efficiency. Generally speaking, a large size (and high density) of the grinding medium is useful since the larger weight of the balls will transfer more impact energy to the powder particles. It has also been reported that the final constitution of the powder is dependent upon the size of the grinding medium used. For example, when balls of 15 mm diameter were used to mill the blended elemental Ti-Al powder mixture, a solid solution of aluminum in titanium was formed. On the other hand, use of 20 and 25 mm diameter balls resulted in a mixture of only the titanium and aluminum phases, even after a long milling duration [8]. In another set of investigations, it has been reported that an amorphous phase could be produced faster in Ti-Al alloys by using steel balls of 3/16" diameter than by using balls of ¾" diameter. In fact, in some cases, an amorphous phase was not produced and only the stable crystalline compound formed when milling was done with large steel balls [30]. In yet another investigation it was reported that an amorphous phase formed only when the Ti-Al powder mixture was milled using either 5 or 8 mm diameter balls; an amorphous phase did not form when 12 mm diameter balls were used for milling. A similar situation was also reported in the Pd-Si system where it was reported that a smaller ball size favored amorphous phase formation [31]. It was suggested that the smaller balls produced intense frictional action, which promoted

the amorphous phase formation. In fact, it appears that ``soft" milling conditions (small ball sizes, lower energies, and lower ball-to-powder ratios) seem to favor amorphization or metastable phase formation [31].Even though most of the investigators generally use only one size of the grinding medium, there have been instances when different sized balls have been used in the same investigation. It has been predicted that the highest collision energy can be obtained if balls with different diameters are used. In the initial stages of milling, the powder being milled gets coated onto the surface of the grinding medium and also gets cold welded. This is advantageous since it prevents excessive wear of the grinding medium and also avoids contamination of the powder due to the wear of the grinding medium. However, the thickness of this layer must be kept to a minimum to avoid formation of a heterogeneous product [32]. But, the disadvantage of this powder coating is that it is difficult to detach this powder and so the powder yield is low. It has been reported that a combination of large and small size balls during milling minimizes the amount of cold welding and the amount of powder coated onto the surface of the balls [33]. Although no specific explanation has been given for the improved yield under these conditions, it is possible that the different sized balls produce shearing forces that may help in detaching the powder from the surface of the balls. Use of grinding balls of the same size in either a round or at bottom vial has been shown to produce tracks. Consequently, the balls roll along a well-defined trajectory instead of hitting the end surfaces randomly. Therefore it is necessary to use several balls, generally a combination of smaller and larger balls to ``randomize" the motion of the balls [34].

(e)Ball to powder ratio: The ratio of the weight of the balls to the powder (BPR), sometimes referred to as charge ratio (CR), is an important variable in the milling process. This has been varied by different investigators from a value as low as 1:1 to as high as 220:1 [35]. Generally speaking, a ratio of 10:1 is most commonly used while milling the powder in a small capacity mill such as a SPEX mill. But, when milling is conducted in a large capacity mill, like an attritor, a higher BPR of up to 50:1 or even 100:1 is used. The BPR has a significant effect on the time required to achieve a particular phase in the powder being milled. The higher the BPR, the shorter is the time C. Suryanarayana / Progress in Materials Science 46 (2001) 1-184 24 required. For example, formation of an amorphous phase was achieved in a Ti-33 at% Al powder mixture milled in a SPEX mill in 7 h at a BPR of 10:1, in 2 h at a BPR of 50:1 and in 1 h at a BPR of 100:1 [36]. At a high BPR, because of an increase in the weight proportion of the balls, the number of collisions per unit time increases and consequently more energy is transferred to the powder particles and so alloying takes place faster. Several other investigators also have reported similar results. It is also possible that due to the higher energy, more heat is generated and this could also change the constitution of the powder. The amorphous phase formed may even crystallize if the temperature rise is substantial. As mentioned earlier, ``soft" conditions (e.g., low BPR values, low speeds of rotation, etc.) of MA produce metastable phases whereas ``hard" condition produce the equilibrium phases. This was first very clearly

demonstrated in the Zr-Co system when an amorphous phase was obtained under ``soft'' milling conditions, while a mixture of the equilibrium crystalline phases was obtained under ``hard'' milling conditions [37]. Similar results were also reported for other alloy systems. For example, a metastable cubic phase was formed at low BPR, while the stable equilibrium tetragonal phase was formed at higher BPR in the mechanically alloyed Cu-In-Ga-Se powder system [38].

(f)Extent of filling the vial: Since alloying among the powder particles occurs due to the impact forces exerted on them, it is necessary that there is enough space for the balls and the powder particles to move around freely in the milling container. Therefore, the extent of filling the vial with the powder and the balls is important. If the quantity of the balls and the powder is very small, then the production rate is very small. On the other hand, if the quantity is large, then there is not enough space for the balls to move around and so the energy of the impact is less. Thus, care has to be taken not to overfill the vial; generally about 50% of the vial space is left empty.

(g)Milling atmosphere: The major effect of the milling atmosphere is on the contamination of the powder. Therefore, the powders are milled in containers that have been either evacuated or filled with an inert gas such as argon or helium. (Nitrogen has been found to react with metal powders and consequently it cannot be used to prevent contamination during milling, unless one is interested in producing nitrides.) High-purity argon is the most common time, but in a nitrogen atmosphere, picked up 4.7 wt% oxygen; a difficult to explain observation. Normally, the loading and unloading of the powders into the vial is carried out inside atmosphere-controlled glove boxes. These glove boxes are usually repeatedly evacuated and refilled with the argon gas. Some investigators have even conducted the milling operation in mills that have been placed inside the evacuated glove boxes. Different atmospheres have been used during milling for specific purposes. Nitrogen or ammonia atmospheres have been used to produce nitrides [39]. Hydrogen atmosphere was used to produce hydrides. The presence of air in the vial has been shown to produce oxides and nitrides in the powder, especially if the powders are reactive in nature. Thus, care has to be taken to use an inert atmosphere during milling. The type of atmosphere also seems to affect the nature of the final phase. For example, it has been shown that when Cr-Fe powder mixtures were milled in different types of atmosphere, the constitution of the final powder was different. When the powder was milled in an argon atmosphere, no amorphous phase formed and Cr peaks remained in the X-ray diffraction pattern. On the other hand, when the powder was milled in either air containing argon or a nitrogen atmosphere, the powder became completely amorphous. Similarly, oxygen was shown to enhance the kinetics of amorphization in the Ni-Nb system [40].

(h)Process control agents: The powder particles get cold-welded to each other, especially if they are ductile, due to the heavy plastic deformation experienced by

them during milling. But, true alloying among powder particles can occur only when a balance is maintained between cold welding and fracturing of particles. A process control agent (PCA) (also referred to as lubricant or surfactant) is added to the powder mixture during milling to reduce the effect of cold welding. The PCAs can be solids, liquids, or gases. They are mostly, but not necessarily, organic compounds, which act as surface-active agents. The PCA adsorbs on the surface of the powder particles and minimizes cold welding between powder particles and thereby inhibits agglomeration. The surface-active agents adsorbed on particle surfaces interfere with cold welding and lower the surface tension of the solid material. Since the energy required for the physical process of size reduction, E is given by

$$E = g * \Delta S$$

Where, g is the specific surface energy and ΔS is the increase of surface area, a reduction in surface energy results in the use of shorter milling times and/or generation of finer powders. A wide range of PCAs has been used in practice at a level of about 1-5 wt% of the total powder charge. The most important of the PCAs include stearic acid, hexane, methanol, and ethanol. A partial listing of the PCAs used in different investigations and their quantities is presented in Table 5. Additionally, other exotic PCAs such as sodium-1,2-bis-(dodecyl carbonyl)ethane-1-sulfonate, lithium- 1,2-bis-dodecyloxy carbonyl sulfasuccinate, diodecyl dimethyl ammonium acetate (DDAA), didocyldimethyl ammonium bromide (DDAB), trichlorotrifluoroethane.

Table 2

Process control agents (PCAs) and the quantities used in different investigations

PCA	Chemical formula	Quantity
Benzene	C6H6	---
C wax	H35C17CONHC2H4NHCOC17H35	1.5 wt%
Ethanol	C2H5OH	4 wt%
Ethyl acetate	CH3CO2C2H5	---
Ethylenebisdistearamide Nopcowax-22 DSP	C2H2-2(C18H36ON)	2 wt%
Graphite	C	0.5 wt%
Heptane	CH3(CH2)5CH3	0.5 wt%

(i)Temperature of milling: The temperature of milling is another important parameter in deciding the constitution of the milled powder. Since diffusion processes are involved in the formation of alloy phases irrespective of whether the final product phase is a solid solution, intermetallic, nanostructure, or an amorphous phase, it is expected that the

temperature of milling will have a significant effect in any alloy system. There have been only a few investigations reported where the temperature of milling has been intentionally varied. This was done by either dripping liquid nitrogen on the milling container to lower the temperature or electrically heating the milling vial to increase the temperature of milling. These investigations were undertaken to study the effect of milling temperature on the variation in solid solubility levels, or to determine whether an amorphous phase or a nanocrystalline structure forms at different temperatures. During the formation of nanocrystals, it was reported that the root mean square (rms) strain in the material was lower and the grain size larger for materials milled at higher temperatures [41]. The extent of solid solubility was reported to decrease at higher milling temperatures. For example, during planetary ball milling of a Cu-37at%Ag powder mixture, it was noted that a mixture of an amorphous and crystalline (supersaturated solid solution) phases was obtained on milling at room temperature; instead, only a Cu-8at%Ag solid solution was obtained on milling the powder at 200°C. Similar results were also reported by others in the Cu-Ag, Zr-Al, and Ni-Ag alloy systems and were explained on the basis of the increased diffusivity and equilibration effects at higher temperatures of milling.

2.3.6.4 Mechanism of alloying: During high-energy milling the powder particles are repeatedly flattened, cold welded, fractured and rewelded. Whenever two steel balls collide, some amount of powder is trapped in between them. Typically, around 1000 particles with an aggregate weight of about 0.2 mg are trapped during each collision. The force of the impact plastically deforms the powder particles leading to work hardening and fracture. The new surfaces created enable the particles to weld together and this leads to an increase in particle size. Since in the early stages of milling, the particles are soft (if we are using either ductile-ductile or ductile-brittle material combination), their tendency to weld together and form large particles is high. A broad range of particle sizes develops, with some as large as three times bigger than the starting particles. The composite particles at this stage have a characteristic layered structure consisting of various combinations of the starting constituents. With continued deformation, the particles get work hardened and fracture by a fatigue failure mechanism and/or by the fragmentation of fragile flakes. Fragments generated by this mechanism may continue to reduce in size in the absence of strong agglomerating forces. At this stage, the tendency to fracture predominates over cold welding. Due to the continued impact of grinding balls, the structure of the particles is steadily refined, but the particle size continues to be the same. Consequently, the inter-layer spacing decreases and the number of layers in a particle increase.
ambient to prevent oxidation and/or contamination of the powder. It has also been noted that oxidation can be generally prevented or minimized in the presence of nitrogen ambient. But, this does not appear to be true when reactive powders such as titanium or its alloy powders are milled. It has been reported that a Ti-48Al-2W (at %) powder milled in an oxygen atmosphere picked up 1.5 wt% oxygen after 20 h of milling. The same powder milled for the same length of

However, it should be remembered that the efficiency of particle size reduction is very low, about 0.1% in a conventional ball mill. The efficiency may be somewhat higher in high-energy ball milling processes, but is still less than 1%.The remaining energy is lost mostly in the form of heat, but a small amount is also utilized in the elastic and plastic deformation of the powder particles.

3. EXPERIMENTAL:

3.1 Sample Preparation: Seven samples of nominal composition of $Al_{75}Si_{15}Ni_{10}$ were prepared by taking a mixture of pure powder of Al (purity ~ 99.0%), Si (purity ~98.0%) & Ni(purity ~90 %) by the process of mechanical milling in a planetary ball mill. Total weight of powder taken was 21gms each and milling was done by using stainless steel balls having diameter of 10 mm. The ball to powder ratio was taken as 10:1 and the milling speed was maintained at 300 rpm. Toluene was used as process control agent (PCA), which filled container slightly more than the half. The vials arranged on a rotating support disk and a special drive mechanism causes them to rotate around their own axes. The centrifugal force produced by the vials rotating around their own axes and that produced by the rotating support disk both act on the vial contents, consisting of material to be ground and the grinding balls. Since the vials and the supporting disk rotate in opposite directions, the centrifugal forces alternately act in like and opposite directions. This causes the grinding balls to run down the inside wall of the vial the friction effect, followed by the material being ground and grinding balls lifting of and traveling freely through the inner chamber of the vial and colliding against the opposing inside wall the impact effect

The milling time for the whole milling process was 50 h. The seven samples were collected from the vial after 0, 5, 10, 20, 30, 40 and 50 h of mechanical alloying and were packed safely in an inert atmosphere. The samples were analyzed by X-ray diffraction (XRD) and scanning electron microscopy (SEM) to determine its microstructural features.

3.2 X-ray diffraction (XRD) : XRD is a rapid analytical technique primarily used for phase identification of a material & can provide information on unit cell dimensions. X-rays are used

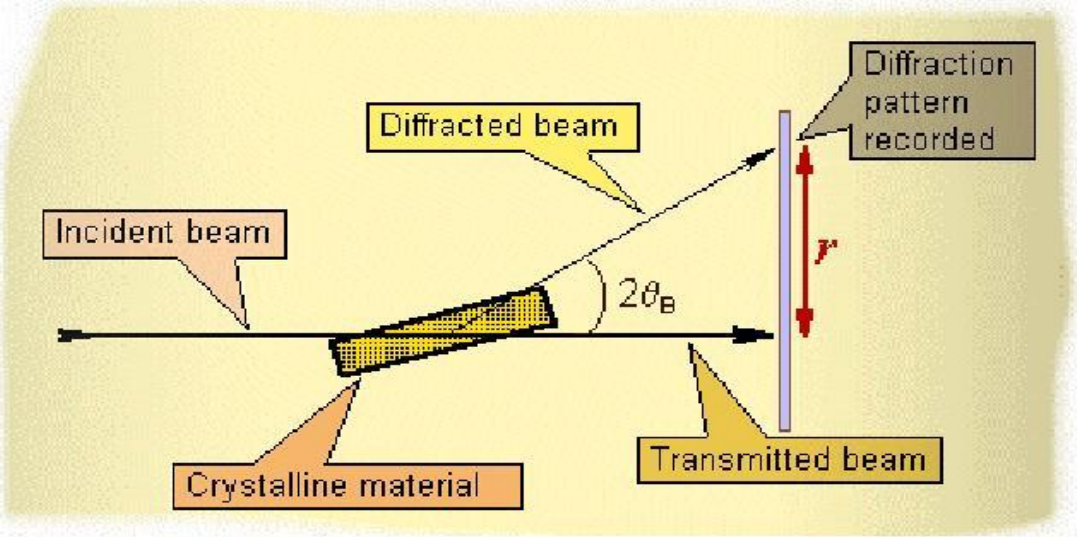

to carry out XRD by causing the phenomenon of diffraction. The atomic planes of a crystal cause an incident beam of X-rays to interfere with one another as they leave the crystal. The phenomenon is called X-ray diffraction. X-rays are generally electromagnetic radiation having wavelength range of 0.01 to 10nm. X-rays are produced whenever high-speed electrons collide with a metal target. To produce x-ray a source of electrons (hot W filament), a high accelerating voltage between the cathode (W) and the anode and a metal target (Cu, Al, Mo, Mg etc). The anode is a water-cooled block of Cu containing desired target metal. Thus the x-rays are generated and are made incident on the sample so that it would cause diffraction. The diffraction phenomenon is governed by Bragg's law

$$n\lambda = 2d.sin\theta$$

Where,

- N is an integer determined by the order given.
- λ is the wavelength of X-rays, and moving electrons, protons and neutrons.
- *d* is the spacing between the planes in the atomic lattice.
- θ is the angle between the incident ray and the scattering planes.

XRD patterns (Intensity(I) vs Bragg angle (2θ)) are obtained and various parameters of a unit crystal are calculated i.e. lattice parameters, crystal strain, crystal size, shape, phase etc. by studying the peak position, peak width & the peak intensity of the XRD

pattern. X-ray diffraction (XRD) analyses were carried out with a Philip's X'pert PRO highresolution X-ray diff- ractometer using Cu (λ=1.54 Å) as the target. The XRD patterns recorded in the 2θ range of 10-90° (step size of 2°, time per step 1 min). The aluminium crystallite sizes and lattice microstrain estimated with the broadening of XRD peaks by Scherrer equation]. The Al lattice parameter was calculated using first 3 Al XRD peaks and the average value is reported.

3.3 Scanning Electron Microscope (SEM): The scanning electron microscope (SEM) is a type of electron microscope that images the sample surface by scanning it with a high-energy beam of electrons in a raster scan pattern. The electrons interact with the atoms that make up the sample producing signals that contain information about the sample's surface topography, composition and other properties such as electrical conductivity. The types of signals produced by an SEM include secondary electrons, back scattered electrons (BSE), characteristic x-rays, light (cathodoluminescence), specimen current and transmitted electrons. These types of signal all require specialized detectors for their detection that are not usually all present on a single machine.

The signals result from interactions of the electron beam with atoms at or near the surface of the sample. In the most common or standard detection mode, secondary electron imaging or SEI, the SEM can produce very high-resolution images of a sample surface, revealing details about 1 to 5 nm in size. Due to the way these images are created, SEM micrographs have a very large depth of field yielding a characteristic three-dimensional appearance useful for understanding the surface structure of a sample. The signals result from interactions of the electron beam with atoms at or near the surface of the sample. In the most common or standard detection mode, secondary electron imaging or SEI, the SEM can produce very high-resolution images of a sample surface, revealing details about 1 to 5 nm in size.

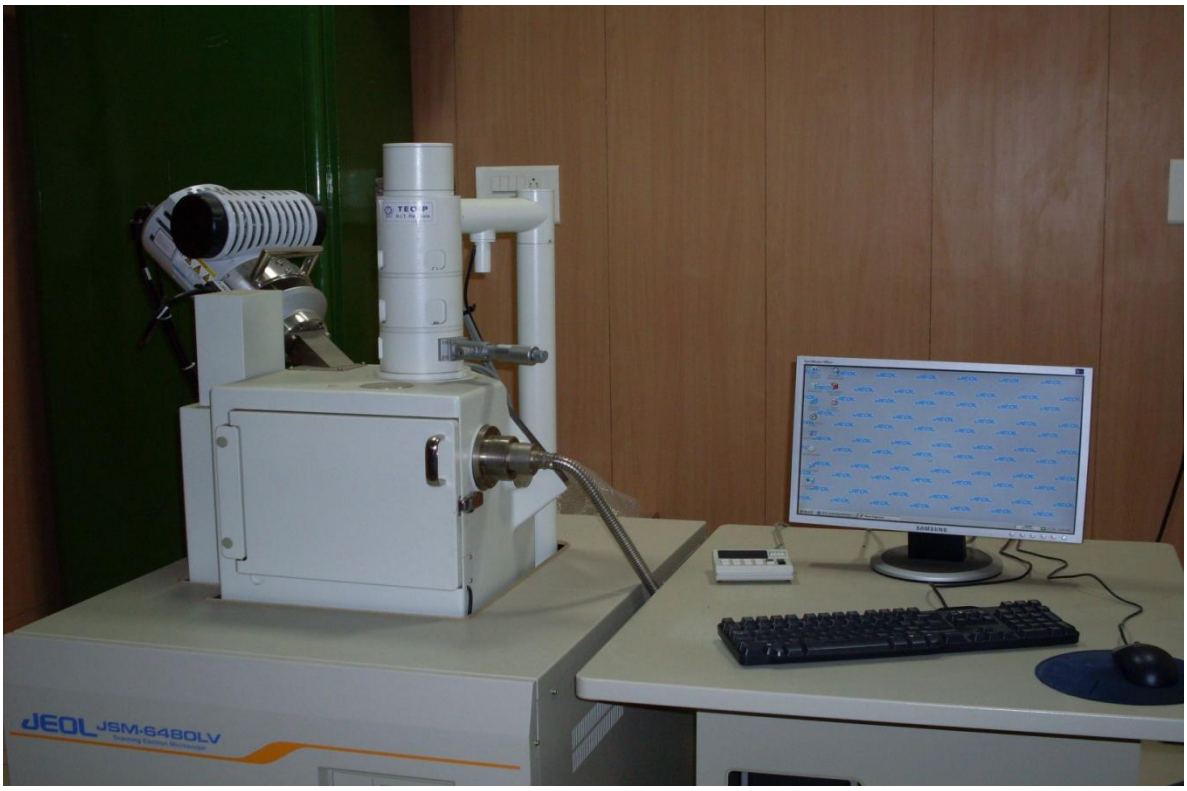

SEM(*JEOL JSM-6480LV)*, NIT Rourkela

The signals result from interactions of the electron beam with atoms at or near the surface of the sample. In the most common or standard detection mode, secondary electron imaging or SEI, the SEM can produce very high-resolution images of a sample surface, revealing details about 1 to 5 nm in size. Due to the way these images are created, SEM micrographs have a very large depth of field yielding a characteristic three-dimensional appearance useful for understanding the surface structure of a sample. This is exemplified by the micrograph of pollen shown to the right. A wide range of magnifications is possible, from about x 25 (about equivalent to that of a powerful hand-lens) to about x 250,000, about 250 times the magnification limit of the best light microscopes. Back-scattered electrons (BSE) are beam electrons that are reflected from the sample by elastic scattering. BSE are often used in analytical SEM along with the spectra made from the characteristic x-rays. Because the intensity of the BSE signal is strongly related to the atomic number (Z) of the specimen, BSE images can provide information about the distribution of different elements in the sample. For the same reason BSE imaging can image colloidal gold immuno-labels of 5 or 10 nm diameter, that would otherwise be difficult or impossible to detect in secondary electron images in biological specimens. Characteristic X-rays are emitted when the electron beam removes an inner shell electron from the sample, causing a higher energy electron to fill the shell and release energy. These characteristic x-rays are used to identify the composition and measure the abundance of elements in the sample.

In a typical SEM, an electron beam is thermionically emitted from an electron gun fitted with a tungsten filament cathode. Tungsten is normally used in thermionic electron guns because it has the highest melting point and lowest vapour pressure of all metals, thereby allowing it to be heated for electron emission, and because of its low cost. Other types of electron emitters include lanthanum hexaboride (LaB_6) cathodes, which can be used in a standard tungsten filament SEM if the vacuum system is upgraded and field emission guns (FEG), which may be of the cold-cathode type using tungsten single crystal emitters or the thermally-assisted Schottky type using emitters of zirconium oxide. The electron beam, which typically has an energy ranging from a few hundred eV to 40 keV, is focused by one or two condenser lenses to a spot about 0.4 nm to 5 nm in diameter. The beam passes through pairs of scanning coils or pairs of deflector plates in the electron column, typically in the final lens, which deflect the beam in the x and y axes so that it scans in a raster fashion over a rectangular area of the sample surface. When the primary electron beam interacts with the sample, the electrons lose energy by repeated random scattering and absorption within a teardrop-shaped volume of the specimen known as the interaction volume, which extends from less than 100 nm to around 5 μm into the surface. The size of the interaction volume depends on the electron's landing energy, the atomic number of the specimen and the specimen's density. The energy exchange between the electron beam and the sample results in the reflection of high-energy electrons by elastic scattering, emission of secondary electrons by inelastic scattering and the emission of electromagnetic radiation, each of which can be detected by specialized detectors. The beam current absorbed by the specimen can also be detected and used to create images o of the distribution of specimen current. Electronic amplifiers of various types are used to amplify the signals which are displayed as variations in brightness on a cathode ray tube. The raster scanning of the CRT display is synchronised with that of the beam on the specimen in the microscope, and the resulting image is therefore a distribution map of the intensity of the signal being emitted from the scanned area of the specimen.

3.4. Energy Dispersive X-ray analysis (EDX): Energy dispersive X-ray spectroscopy (EDS, EDX or EDXRF) is an analytical technique used for the elemental analysis or chemical characterization of a sample. It is one of the variants of XRF. As a type of spectroscopy, it relies on the investigation of a sample through interactions between electromagnetic radiation and matter, analyzing x-rays emitted by the matter in response to being hit with charged particles. Its characterization capabilities are due in large part to the fundamental principle that each element has a unique atomic structure allowing x-rays that are characteristic of an element's atomic structure to be identified uniquely from each other.

To stimulate the emission of characteristic X-rays from a specimen, a high energy beam of charged particles such as electrons or protons (see PIXE), or a beam of X-rays, is

focused into the sample being studied. At rest, an atom within the sample contains ground state (or unexcited) electrons in discrete energy levels or electron shells bound to the nucleus. The incident beam may excite an electron in an inner shell, ejecting it from the shell while creating an electron hole where the electron was. An electron from an outer, higher-energy shell then fills the hole, and the difference in energy between the higher-energy shell and the lower energy shell may be released in the form of an X-ray. The number and energy of the X-rays emitted from a specimen can be measured by an energy dispersive spectrometer. As the energy of the X-rays emitted from a specimen can be measured by an energy dispersive spectrometer. As the energy of the X-rays is characteristic of the difference in energy between the two shells, and of the atomic structure of the element from which they were emitted, this allows the elemental composition of the specimen to be measured.

4. RESULTS AND DISSCUSSION:

4.1. Structural Characterization of Mechanically Alloyed Powders By XRD Analysis:

Fig (1) shows XRD patterns of the $Al_{75}Si_{15}Ni_{10}$ alloy for different milling times. At the early stage of milling all Al, Si and Ni peaks were observed. Towards the end of milling only Si was observed. The peak intensity decreased with increasing milling time with broadening. It can be observed that after 20h of milling Al and Ni peaks decreased drastically and disappeared gradually. The presence of Al-Ni, Ni-Si intermetallics have revealed to be present in a negligible amount from the diffraction pattern, which suggests only complete solubility. The significant broadening of the Al peaks may be due to the reduction and refinement of the grain size and the increase in the internal strain induced from the repeated fracturing and welding process during mechanical alloying

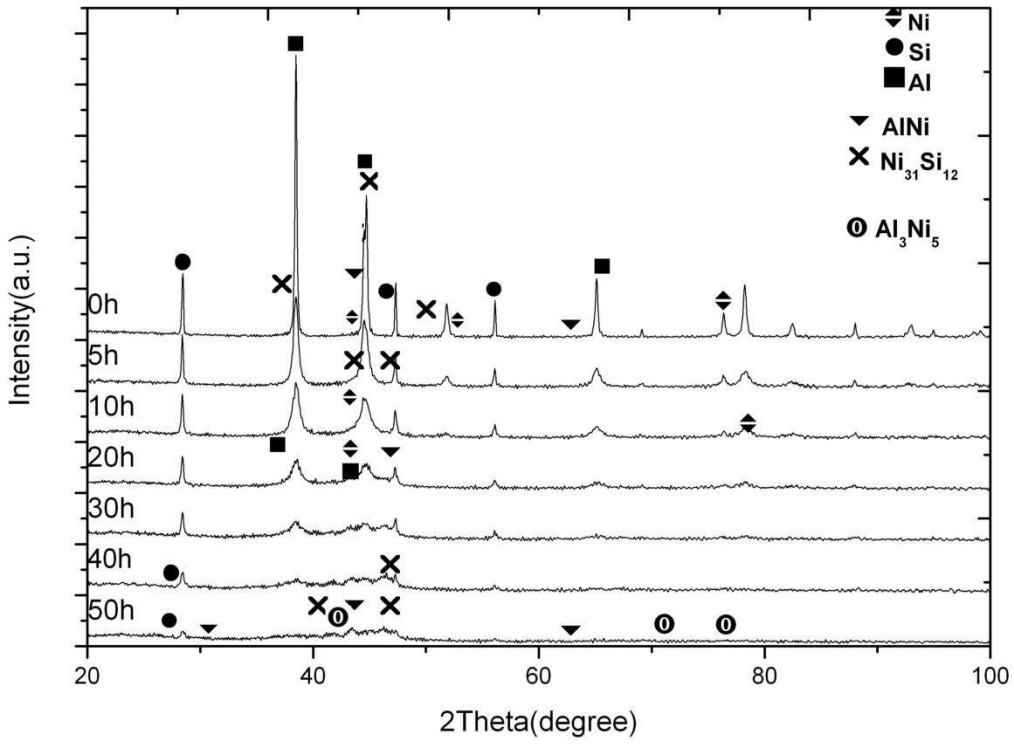

Fig (1): XRD patterns of $Al_{75}Si_{15}Ni_{10}$ alloy with progress of MA.

Crystallite size, lattice microstrain and lattice parameter of each alloy powder has calculated from the XRD peak broadening. Following Scherrer equation, the crystallite size and the lattice strain have been determined for milled samples.

$$\Gamma = K\lambda / \beta\cos\theta$$

Where, Γ - mean crystallite dimension
K - Shape Factor
λ- X-ray wavelength
β- FWHM (in radians)
θ - Bragg Angle

The lattice parameter value were calculated from the peak positions of Al from XRD pattern by extrapolation of 'a_{Al}' against $\cos^2\theta/\sin\theta$ plot to $\cos\theta = 0$ [42].

Fig (2) shows variation of (a) crystallite size (b) lattice microstrain and (c) lattice parameter of Al-rich solid solution in $Al_{75}Si_{15}Ni_{10}$ alloy with milling time. There was a continuous reduction in the crystallite size during different stages of mechanical milling and it remained almost constant after 25 h of milling.

The crystallite size estimated from the XRD analysis of the powder was close to 30 nm. The lattice strain induced increased rapidly during initial stages of mechanical milling up to 25 h and slowly became nearly constant with further milling. The induced lattice strain (%) is ~0.22 during zero hour and increases to ~0.95. The estimated lattice strain (%) was found ~0.45. This suggests that major structural changes and dissolution of the alloying elements almost completed by 25 h, and further milling refined the product by MA.

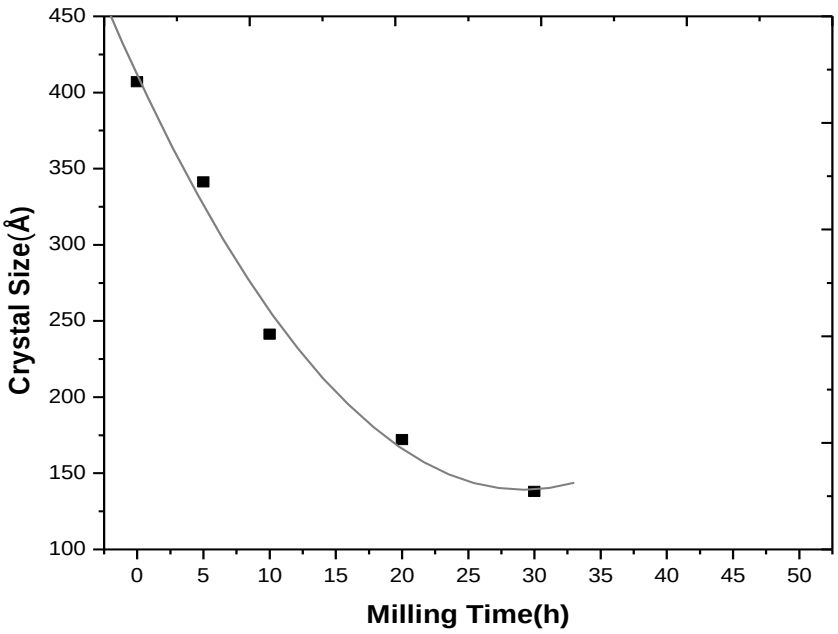

Fig 2 (a) : Variation of crystallite size
of Al-rich solid solution in $Al_{75}Si_{15}Ni_{10}$ alloy with milling time.

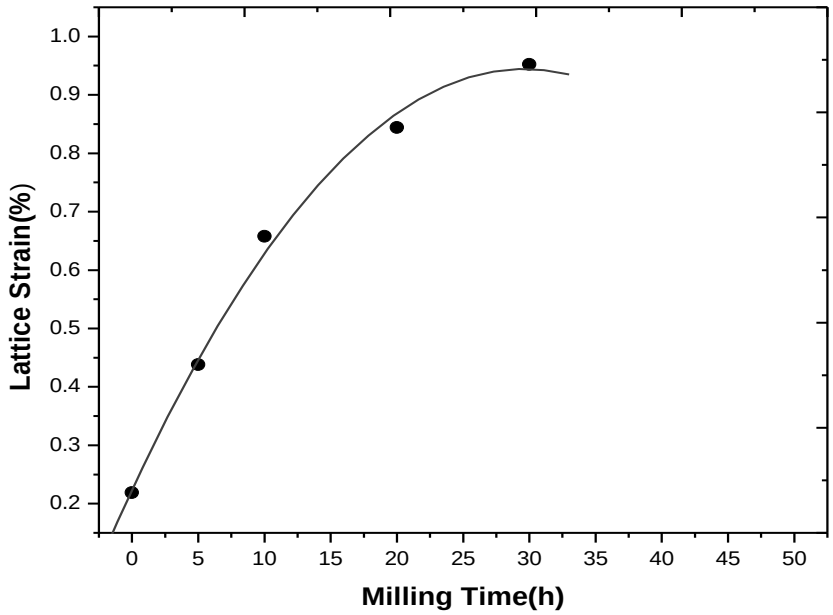

Fig 2 (b) : Variation of (b) lattice microstrain
of Al-rich solid solution in $Al_{75}Si_{15}Ni_{10}$ alloy with milling time.

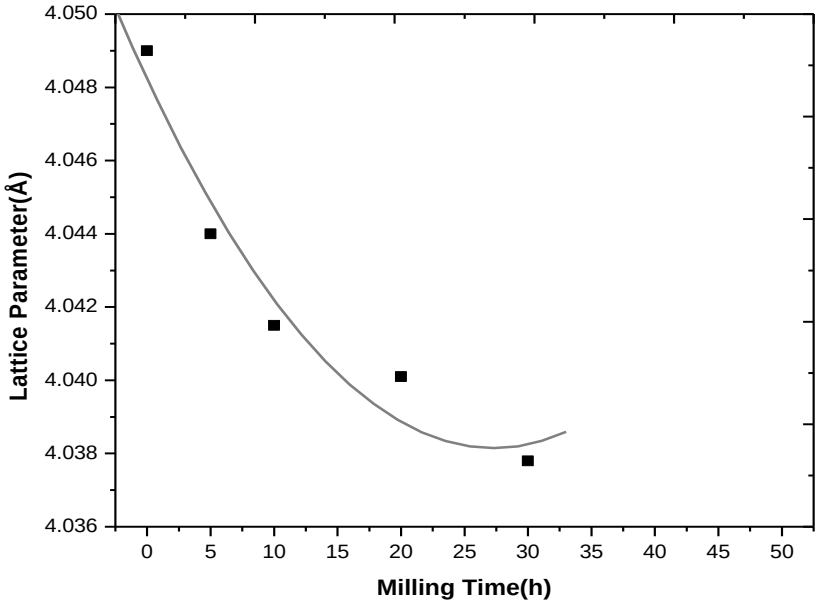

Fig 2(c)

Fig 2(c) : Variation of lattice parameter
of Al-rich solid solution in $Al_{75}Si_{15}Ni_{10}$ alloy with milling time.

The lattice parameter of Al-rich solid solution (a_{Al}) was ~4.045 Å and showed a sharp decreasing value with the progress of milling varying from 4.049 Å to 4.0381 Å. This is because of the entrance of Si and Ni atoms into the lattice of the Al which causes distortion in it. The atomic radii of Ni (0.135 nm) and Si (0.117 nm) are smaller than that of Al (0.14318 nm). The atomic size difference is within the 15% of the atomic radius of Al [43]. The smaller Si and Ni atoms were expected to enter into the solid solution of Al during the early stage of mechanical alloying. The formation of nanocrystalline structures during milling may also enhance dissolution of Si and Ni in Al. because of formation of amorphous alloy. The change in the above mentioned parameters were determined up to 30 h of milling as on further milling Al peaks vanishes.

4.2. Morphology of Powdered Samples

Fig 3 shows changes in the morphology of $Al_{75}Si_{15}Ni_{10}$ powders after mechanical alloying for (a) 5 h; (b) 20 h; and (c) 50 h at 1000 X magnification. Initially at 0 h a coarse particle structure can be seen. After 20 h of milling course-layered structure has appeared which may be due to repeated cold welding and fracturing of the powder particles. The coarse layered structure gradually refined with the proceeding of milling as fracture predominates cold welding, because of strain hardening of materials. Then on further milling particle size decreases. Finally, after 50h of milling a finer refined structure has obtained.

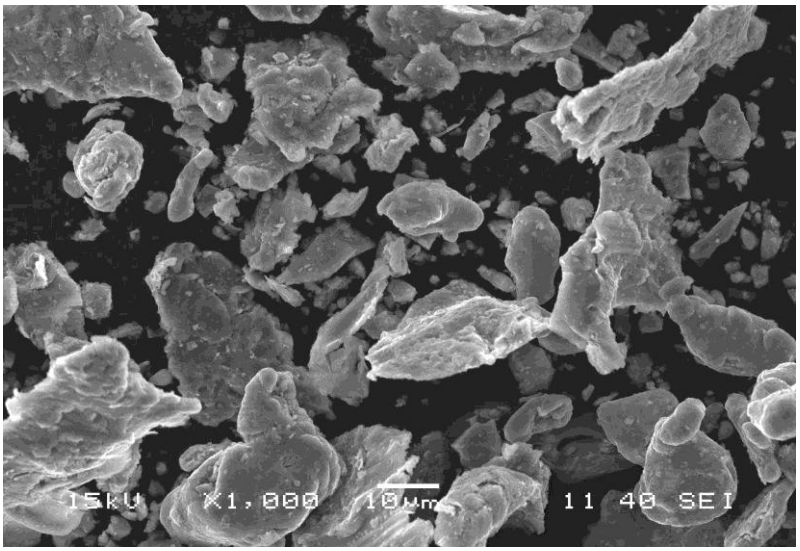

Fig 3(a) : SEM images of $Al_{75}Si_{15}Ni_{10}$ powders milled for (a) 5 h

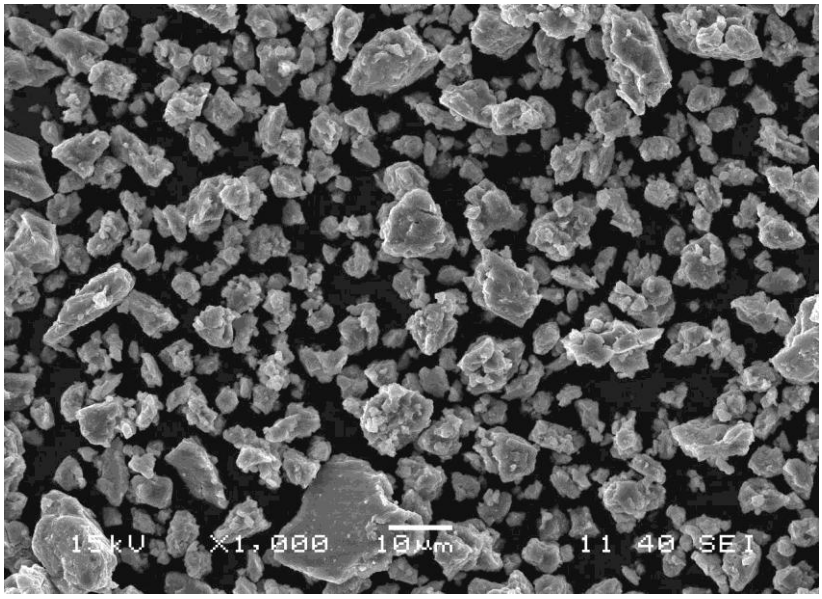

Fig 3(b) : SEM images of $Al_{75}Si_{15}Ni_{10}$ powders milled for 20 h

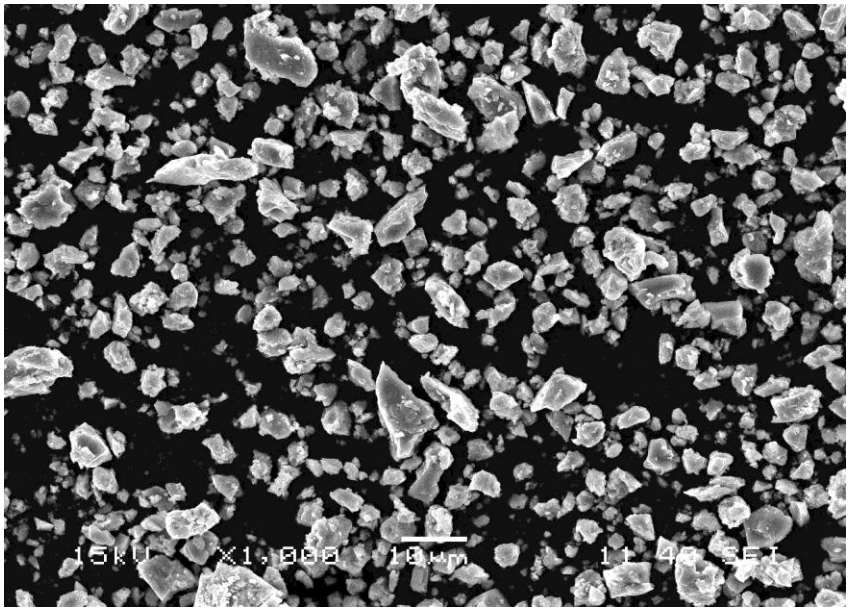

Fig 3(c)

Fig 3(c) : SEM images of $Al_{75}Si_{15}Ni_{10}$ powders milled for 50 h

4.3 EDX Analysis:

EDX (Energy Dispersive X-ray) analysis was done along with SEM, in order to see the chemical composition of each particle of the powders. As a type of spectroscopy, it relies on the investigation of a sample through interactions between electromagnetic radiation and matter, analyzing x-rays emitted by the matter in response to being hit with charged particles. I It was used to determine the composition of powder particles after 50 h of milling and to know whether proper alloying has been achieved or not.

Element	$Al_{75}Si_{15}NI_{10}$	Atomic%
Al	75	81.35
Si	15	12.50
Ni	10	6.15

Table 1: EDX analysis of $Al_{75}Si_{15}Ni_{10}$ powder after MA for 0 h

Element	$Al_{75}Si_{15}NI_{10}$	Atomic%
Al	75	79.33
Si	15	13.15
Ni	10	7.52

Table 2: EDX analysis of $Al_{75}Si_{15}Ni_{10}$ powder after MA for 20 h

Element	$Al_{75}Si_{15}NI_{10}$	Atomic%
Al	75	74.33
Si	15	16.15
Ni	10	9.52

Table 3: EDX analysis of $Al_{75}Si_{15}Ni_{10}$ powder after MA for 50 h

The EDX analysis of $Al_{75}Si_{15}Ni_{10}$ powders after 50h of milling has shown in Table. It shows atomic % and weight % which shows a homogeneous chemical composition has obtained for sample milled for 50 h. The atomic % of Si and Ni were found slightly greater and lesser respectively during the process of MA.

5. CONCLUSION:

From the present investigation on the formation of phases in Al-Si-Ni alloy developed by MA, the following conclusions can be made:

1.The mechanical alloying of $Al_{75}Si_{15}Ni_{10}$ up to 50 h resulted partially amorphous structure along with some intermetallic phases.

2. The crystallite size was ~14 nm and lattice microstrain (%) increased to ~0.952 after 30 h of milling.

3. The lattice parameter of Al-rich solid solution decreased with increase in milling time up to 30 h indicating the progressive dissolution of Si and Ni in Al.

4. The lattice parameter (a_{Al}) of 30 h milled product was found to be ~4.0381 Å.

5. EDX analysis revealed that a homogeneous nanostructure was formed during MA of $Al_{75}Si_{15}Ni_{10}$ up to 50 h.

5.1 Scope for Future Work:

1. The present work leaves a wide scope for future investigators to explore many other aspects like TEM studies to determine directly the structured formed by MA.

2. Consolidation of this nanostructure keeping nanofeatures may result high strength bulk nanocomposite.

6. REFERENCES:-

1- C.Suryanarayana, Nanocrystalline materials review, 1995, 40:22, 41-64.

2- Schuh, Christopher, Nieh, T.G. (2003), Hardness & abrasion Resistance of nanocrystalline Ni alloys, Mat.Soc.Symp.Proc.740.

3- A.P.Tsai, A.Inoue & T.Masumoto Metall.Trans.A19 (1988)1369.

4-Polmear, I.J.Metallurgy of light alloys,Third Ed.,pp. 305-314, 1995.

5-A.Inoue, H.M.Kimura, K.Sasamori, Masumoto,Mater.Trans, JIM 36(1995)6.

6-W.F. Gale, T.C.Totemeier,Smithells metals reference book,8th edition,Elsevier,Oxford,1997.

7-T.H.Lee, A.Inoue, T.Mausmoto,scripta metal, 475, 1997.

8-J.Latuch, G.Cieslac,T.Kulik,Journal of alloys and compounds, 434-435, 272-274, 2007.

9-W.H.Hunt,Jr.J.,Powder Metal,36-60, 51-60, 2000.

12-Gleiter H.Acta Mater 2000; 1-29.

10-W.D. Callister,Fundamental of material science and Engg.,2nd edition,Wiley & Sons.

11-Sanders PG,Eastmen JA, Weertman JR,Acta Mater 1997;45;4019.

12-Swygenhoven HV,Caro A,Nanostuctured Mater 1997;6;1012-27.

13-Conrad H,Narayan J,Acta mater 2002;50:5067.

14-Iyer RS,Frey CA,Sastry SML,Walker BE,Mater Sci Eng A-Phy Met Mater Sci 1998;29:2261-71.

15- Jia D, Ramesh KT, Ma E. Scripta Mater 2000;42:73.

16- Whitney AB, Sanders PG, Weertman JR. Scripta Metall Mater 1995;33:2025–30.

17- Gleiter H. Nanocrystalline materials. Prog Mater Sci 1989;33:223–315.

18- Niemann GW, Weertman JR, Siegel RW. Scripta Metall Mater 1990;24:145.

19-Erb U. Nanostruct Mater 1995;6:533–8.

20-Lu K. Mater Sci Eng 1996;R16:161–221.

21- Rack HJ, Cohen M. In.uence of recovery on the tensile behavior of highly-strained iron alloys. In: Murr LE, Stein C, editors. Fron Mat Sci 1976:365.

22- Furukawa M, Berbon PB, Horita Z, Nemoto M, Tsenev NK, Valiev RZ, et al. Production of ultra.negrained metallic materials using an intense plastic straining technique. Towards Innovat Superplast I 1997;233:177–84.

23- Bloor D, Brook RJ, Flemings MC, Mahajan S, editors. The encyclopedia of advanced materials. Oxford: Pergamon Press, 1994.

24- Martin G, Bellon P. Solid State Phys 1997;50:189-331112-Koch CC. In: Cahn RW, editor. Processing of metals and alloys, vol. 15 of materials science and technology - a comprehensive treatment. Weinheim, Germany: VCH Verlagsgesellschaft GmbH, 1991. p. 193±245

25-Ivanov E. Mater Sci Forum 1992;88-90:475-80.

26- Di LM, Bakker H. J Phys C: Condens Matter 1991;3:3427-32.

27- Kaloshkin SD, Tomlin IA, Andrianov GA, Baldokhin UV, Shelekhov EV. Mater Sci Forum 1997;235-238:565-70.

28- Calka A, Nikolov JI, Ninham BW. In: deBarbadillo JJ, et al., editors. Mechanical alloying for structural applications. Materials Park, OH: ASM International, 1993. p. 189-95.

29- Calka A, Radlinski AP. Mater Sci and Engng 1991;A134:1350-3.

30- Watanabe R, Hashimoto H, Park Y-H. In: Pease III LF, Sansoucy RJ, editors. Advances in powder metallurgy 1991, vol. 6. Princeton, NJ: Metal Powder Industries Federation, 1991. p.119-30.

31- Park Y-H, Hashimoto H, Watanabe R. Mater Sci Forum 1992;88-90:59-66.

32- Liebermann HH. Amorphous metallic alloys. In: Luborsky, FE, editor; 1988. p. 26.

33- Takacs L, Pardavi-Horvath M. J Appl Phys 1994;75:5864-6.

34- Takacs L. In: Suryanarayana C, et al., editors. Processing and properties of nanocrystalline materials. Warrendale, PA: TMS, 1996. p. 453-64.

35- Kis-Varga, Beke DL. Mater Sci Forum 1996;225-227:465-70.

36- Suryanarayana C, Chen GH, Froes FH. Scripta Metall Mater 1992;26:1727-32.

37- Gerasimov KB, Gusev AA, Ivanov EY, Boldyrev VV. J Mater Sci 1991;26:2495-500.

38- Suryanarayana C, Ivanov E, Noufi R, Contreras MA, Moore JJ. J Mater Res 1999;14:377-83.

39- Guo W, Iasonna A, Magini M, Martelli S, Padella F. J Mater Sci 1994;29:2436-44.

40-Lee PY, Koch CC. J Non-Cryst Solids 1987;94:88-100.

41- Hong LB, Bansal C, Fultz B. Nanostructured Mater 1994;4:949-56.

42-Cullity B.D., Elements of X-ray Diffraction,2nd ed., Addison Wesley, Reading,MA, 1978, 350.

43- Brandes E.A., Brook G.B. (Editor), Smithells Metals Reference Book. 7th Edition.1992, pp 11-27.